arXiv:1104.1418v2 [hep-ph] 20 Jun 2011

$\mathcal{O}(\alpha_s v^2)$ correction to pseudoscalar quarkonium decay to two photons

Yu Jia*,[1,2] Xiu-Ting Yang†,[1] Wen-Long Sang‡,[2,3] and Jia Xu§[1]

[1] *Institute of High Energy Physics, Chinese Academy of Sciences, Beijing 100049, China*

[2] *Theoretical Physics Center for Science Facilities, Chinese Academy of Sciences, Beijing 100049, China*

[3] *Department of Physics, Korea University, Seoul 136-701, Korea*

(Dated: February 17, 2022)

Abstract

We investigate the $\mathcal{O}(\alpha_s v^2)$ correction to the process of pseudoscalar quarkonium decay to two photons in nonrelativistic QCD (NRQCD) factorization framework. The short-distance coefficient associated with the relative-order v^2 NRQCD matrix element is determined to next-to-leading order in α_s through the perturbative matching procedure. Some technical subtleties encountered in calculating the $\mathcal{O}(\alpha_s)$ QCD amplitude are thoroughly addressed.

PACS numbers: *12.38.-t, 12.38.Bx, 13.20.Gd, 13.40.Hq, 14.40.Gx*

* E-mail: jiay@ihep.ac.cn
† E-mail: yangxt@ihep.ac.cn
‡ E-mail: swlong@korea.ac.kr
§ E-mail: xuj@ihep.ac.cn

I. INTRODUCTION

Quarkonium inclusive annihilation decays are historically among the earliest applications of perturbative quantum chromodynamics (QCD) [1–4]. At present, it is widely accepted that these quarkonium inclusive decay processes can be systematically described by the nonrelativistic QCD (NRQCD) factorization approach [5], which is based on the effective-field-theory formalism and directly linked with the first principles of QCD.

In NRQCD factorization approach, the inclusive decay rate can be systematically expressed as the sum of product of short-distance coefficients and the NRQCD operator matrix elements. The short-distance coefficients encode the hard effects of quark and antiquark annihilation at length scale of order $1/m$ (m denotes the mass of heavy quark), which therefore can be accessed by perturbation theory owing to asymptotic freedom of QCD. In contrast, the NRQCD matrix elements are sensitive to the nonperturbative dynamics that occurs at distance of $1/mv$ or longer (v denotes the typical (anti-)quark velocity inside a quarkonium). An important feature of these nonperturbative matrix elements is that they are universal, and satisfy a definite power-counting in v. This attractive feature endows the NRQCD factorization approach with a controlled predictive power.

Among the quarkonium annihilation decay processes, the simplest and cleanest are the quarkonium electromagnetic decays, exemplified by vector quarkonium decay to a lepton pair and pseudoscalar quarkonium decay to two photons. Both of these two processes have been comprehensively studied in theory and experiment for decades. In this work, we will address the $\mathcal{O}(\alpha_s v^2)$ correction to the latter process in NRQCD factorization context. We note that investigations on this process from other approaches are also available (e.g., see [6–8]).

We will generically label a pseudoscalar quarkonium by η_Q, where Q can stand for the c or the b quark. Through relative order-v^4, the NRQCD factorization formula for the decay rate of $\eta_Q \to \gamma\gamma$ reads [9, 10]:

$$\begin{aligned}
\Gamma[\eta_Q \to \gamma\gamma] \;=\; & \frac{F(^1S_0)}{m^2}\left|\langle 0|\chi^\dagger\psi|\eta_Q\rangle\right|^2 + \frac{G(^1S_0)}{m^4}\mathrm{Re}\left\{\langle\eta_Q|\psi^\dagger\chi|0\rangle\langle 0|\chi^\dagger(-\tfrac{i}{2}\overleftrightarrow{\mathbf{D}})^2\psi|\eta_Q\rangle\right\} \\
& + \frac{H^1(^1S_0)}{m^6}\langle\eta_Q|\psi^\dagger(-\tfrac{i}{2}\overleftrightarrow{\mathbf{D}})^2\chi|0\rangle\langle 0|\chi^\dagger(-\tfrac{i}{2}\overleftrightarrow{\mathbf{D}})^2\psi|\eta_Q\rangle \\
& + \frac{H^2(^1S_0)}{m^6}\mathrm{Re}\left\{\langle\eta_Q|\psi^\dagger\chi|0\rangle\langle 0|\chi^\dagger(-\tfrac{i}{2}\overleftrightarrow{\mathbf{D}})^4\psi|\eta_Q\rangle\right\} + O(v^6\Gamma), \qquad (1)
\end{aligned}$$

where ψ and $\chi^\dagger$ represent Pauli spinor fields that annihilate the heavy quark Q and heavy antiquark $\overline{Q}$, respectively.

The short-distance coefficients F, G, H in (1) are

$$F(^1S_0) = 2\pi e_Q^4 \alpha^2 \left[1 + C_F \frac{\alpha_s}{\pi}\left(\frac{\pi^2}{4} - 5\right) + \mathcal{O}(\alpha_s^2)\right], \tag{2a}$$

$$G(^1S_0) = -\frac{8\pi e_Q^4 \alpha^2}{3}\left[1 + \mathcal{O}(\alpha_s)\right], \tag{2b}$$

$$H^1(^1S_0) + H^2(^1S_0) = \frac{136\pi e_Q^4 \alpha^2}{45}\left[1 + \mathcal{O}(\alpha_s)\right], \tag{2c}$$

where ee_Q denotes the electric charge of the heavy quark Q. The $\mathcal{O}(\alpha_s)$ correction to $F(^1S_0)$ was first computed in [11–13]. An incomplete $\mathcal{O}(\alpha_s^2)$ correction to this coefficient has also been available about a decade ago [14], which indicates an uncomfortably large negative correction. The coefficient $G(^1S_0)$ is associated with the order-v^2 matrix element, whose tree-level value has been known long ago [15]. Recently, the tree-level coefficients $H(^1S_0)$ associated with the order-v^4 matrix elements are also available for the first time [9, 10]. Initially only the combination of two $\mathcal{O}(v^4)$ coefficients was given [9], as shown in (2c). Later Ref. [10] was able to determine these two coefficients separately: $H^1(^1S_0) = \frac{20\pi e_Q^4 \alpha^2}{9}$ and $H^2(^1S_0) = \frac{4\pi e_Q^4 \alpha^2}{5}$.

In recent years there have also been many phenomenological investigations on the nonperturbative NRQCD matrix elements for the pseudoscalar quarkonium state [16–18]. Most of them focus on the matrix elements at lowest order (LO) and next-to-leading order (NLO) in v^2. Comparing equation (1) truncated at order v^2 with the measured decay rate of $\eta_c \to \gamma\gamma$, some authors are able to fit the first two NRQCD matrix elements of η_c and find they roughly obey the velocity counting rules [16, 17] [1].

By far, the $\mathcal{O}(\alpha_s^2 v^0)$ contribution [14] and $\mathcal{O}(\alpha_s^0 v^4)$ contribution [9, 10] to the decay rate of $\eta_Q \to \gamma\gamma$ are known. Assuming $\alpha_s(m) \sim v^2$, one may naturally wonder what is the actual size of the $\mathcal{O}(\alpha_s v^2)$ correction. In order to answer this question, one needs first know the $\mathcal{O}(\alpha_s)$ correction to the short-distance coefficient $G(^1S_0)$. It is the purpose of this work to compute this correction through the perturbative matching method.

The remainder of this paper is organized as follows. In section II, we outline the perturbative matching strategy which can be utilized to deduce the NRQCD short-distance

[1] The measured partial width of $\eta_c \to \gamma\gamma$ seems to have changed significantly in past few years, though the full width of η_c almost remains intact. For example, the branching fraction of this decay channel was reported to be $(2.4^{+1.1}_{-0.9}) \times 10^{-4}$ in PDG 2008 edition [19]. But this value has reduced to $(6.3 \pm 2.9) \times 10^{-5}$ in the latest PDG 2010 edition [20]. This may cast some shadow on the reliability of the fitted values for η_c NRQCD matrix elements by using older data [16, 17].

coefficients for our process. In section III, we elaborate on some technical issues encountered in calculating the $\mathcal{O}(\alpha_s)$ correction to $Q\overline{Q}(^1S_0) \to \gamma\gamma$ with the covariant projection approach. In particular, we specify the prescription of γ_5 in dimensional regularization adopted in this work. We also mention some technical ambiguities about extracting the S-wave amplitude. In section IV, we then employ the covariant projection technique to compute the $Q\overline{Q}(^1S_0) \to \gamma\gamma$ amplitude to NLO in α_s. The corresponding $\mathcal{O}(\alpha_s)$ calculation in the NRQCD side is presented in section V. In section VI, by comparing the NLO QCD amplitude and the respective NRQCD amplitude, we determine the first two short-distance coefficients in (1) through order α_s. Finally in section VII, we present a brief summary. The appendix is devoted to enumerating the analytic expressions of the one-loop scalar integrals encountered in the calculation of the NLO QCD correction to $Q\overline{Q}(^1S_0) \to \gamma\gamma$.

II. THE METHOD OF DEDUCING THE SHORT-DISTANCE COEFFICIENTS

In many effective field theories, it is a standard procedure to determine the short-distance coefficient through the matching procedure. We will follow this orthodox method in this work. Our calculation is in close analogy with Ref. [21], where the $\mathcal{O}(\alpha_s v^2)$ correction for $J/\psi \to e^+e^-$ has been deduced also using the matching approach.

It is worth mentioning that the alternative, even more efficient way of deducing the short-distance coefficients exists, exemplified by the *method of region* developed by Beneke and Smirnov [22]. This approach allows one to dissect the loop integral for quarkonium annihilation process into four distinct regions: *hard*, *soft*, *potential* and *ultrasoft*. The short-distance coefficient only receives the contribution from the hard region, while the NRQCD effective theory characterizes the dynamics from the three low-energy regions. To determine the short-distance coefficient, one can either directly compute the hard region contribution order by order in v expansion, or by first calculating the full QCD diagram, then subtracting the contributions from three low energy regions. The second strategy turns out to have some great technical advantage, which enables one to deduce a class of relativistic corrections to arbitrary orders in v^2 with ease. Following this spirit, there have recently been progresses in inferring the all-order-in-v^2 corrections to $J/\psi \to e^+e^-$ [23] and $B_c \to e\bar{\nu}_e$[24].

A. NRQCD factorization formula for the decay amplitude and width

Let us label the momenta of η_Q and two photons by P, k_1 and k_2, and the polarization vectors of two photons by ε_1 and ε_2, respectively. The Lorentz and parity invariance dictates the amplitude of $\eta_Q \to \gamma\gamma$ uniquely of the structure $\epsilon_{\alpha\beta\mu\nu}P^\alpha k_1^\beta \varepsilon_1^{*\mu}\varepsilon_2^{*\nu}$. For the problem at hand, it is most natural to work in the η_Q rest frame. In this frame, the amplitude is then proportional to the kinematic invariant $\mathbf{k}_1 \cdot \boldsymbol{\varepsilon}_1^* \times \boldsymbol{\varepsilon}_2^*$.

When considering quarkonium electromagnetic annihilation decay, one can directly invoke NRQCD factorization at the amplitude level. We need only retain those NRQCD color-singlet operator matrix elements that connect the vacuum to the η_Q state. To the order of desired accuracy, one expects that the following factorization formula holds:

$$\mathcal{A}[\eta_Q \to \gamma\gamma] \;=\; \hat{\mathbf{k}}_1 \cdot \boldsymbol{\varepsilon}_1^* \times \boldsymbol{\varepsilon}_2^* \left[c_0 \langle 0|\chi^\dagger \psi|\eta_Q\rangle + \frac{c_2}{m^2}\langle 0|\chi^\dagger (-\tfrac{i}{2}\overleftrightarrow{\mathbf{D}})^2 \psi|\eta_Q\rangle + \mathcal{O}(v^4)\right], \tag{3}$$

where c_i $(i = 0, 2)$ signify the short-distance coefficients associated with the NRQCD matrix elements at LO and NLO in v^2. It is especially convenient in this work to adopt the nonrelativistic normalization for η_Q state in both sides of (3). In addition, we have explicitly factored out the kinematic invariant, which is represented by a dimensionless Lorentz pseudoscalar,

$$\hat{\mathbf{k}}_1 \cdot \boldsymbol{\varepsilon}_1^* \times \boldsymbol{\varepsilon}_2^* \;=\; -\frac{2}{M_{\eta_Q}^2}\epsilon_{\alpha\beta\mu\nu}P^\alpha k_1^\beta \varepsilon_1^{*\mu}\varepsilon_2^{*\nu}, \tag{4}$$

in the right-hand side of (3), where $\hat{\mathbf{k}}_1 = \mathbf{k}_1/|\mathbf{k}_1|$ is a unit vector. The separation of this kinematic factor renders c_i $(i = 0, 2)$ to bear a very simple form.

Squaring the amplitude in (3), summing over the polarizations of photons, and integrating over the phase space and accounting for the indistinguishability of two photons, we can express the decay rate of $\eta_Q \to \gamma\gamma$ as

$$\begin{aligned}\Gamma[\eta_Q \to \gamma\gamma] \;&=\; \frac{1}{2!}\int \frac{d^3k_1}{(2\pi)^3 2k_1^0}\frac{d^3k_2}{(2\pi)^3 2k_2^0}(2\pi)^4\delta^{(4)}(P-k_1-k_2)\sum |\mathcal{A}[\eta_Q \to \gamma\gamma]|^2 \\ &=\; \frac{1}{8\pi}\left| c_0\langle 0|\chi^\dagger\psi|\eta_Q\rangle + \frac{c_2}{m^2}\langle 0|\chi^\dagger(-\tfrac{i}{2}\overleftrightarrow{\mathbf{D}})^2\psi|\eta_Q\rangle + \cdots\right|^2, \end{aligned}\tag{5}$$

where the formula $\sum_{\text{Pol}} \left|\hat{\mathbf{k}}_1 \cdot \boldsymbol{\varepsilon}_1^* \times \boldsymbol{\varepsilon}_2^*\right|^2 = 2$ has been used.

Comparing (5) with (1), one can express the short-distance coefficients $F(^1S_0)$ and $G(^1S_0)$ that appear in (1), the standard NRQCD factorization formula for the decay rate, in terms

of c_0 and c_2:

$$F(^1S_0) = \frac{m^2}{8\pi}|c_0|^2, \tag{6a}$$

$$G(^1S_0) = \frac{m^2}{4\pi}\mathrm{Re}[c_0 c_2^*]. \tag{6b}$$

The goal of this work is to determine $G(^1S_0)$ through the order α_s. Therefore, we first need determine both of the coefficients c_0 and c_2 to order α_s.

B. Matching at the amplitude level

To determine the values of c_0 and c_2, we follow the moral that these short-distance coefficients, encapsulating the *hard* quantum fluctuations that occur at the length scale $\sim 1/m$, are insensitive to the long-distance hadronic dynamics. As a convenient calculational device, one can replace the physical η_Q meson by a free $Q\overline{Q}$ pair of the quantum number $^1S_0^{[1]}$, so that both the full amplitude, $\mathcal{A}[Q\overline{Q}(^1S_0^{[1]}) \to \gamma\gamma]$, and the NRQCD operator matrix elements can be accessed by perturbation theory. The short-distance coefficients c_i then can be solved by equating the QCD amplitude $\mathcal{A}$ and the corresponding NRQCD amplitude $\mathbb{A}_{\mathrm{NRQCD}}$, order by order in α_s. This procedure is commonly referred to as *perturbative matching*. Analogous to (3), one can write down the pertubative matching formula for the $Q\overline{Q}(^1S_0^{[1]}) \to \gamma\gamma$ process:

$$\mathcal{A}[Q\overline{Q}(^1S_0^{[1]}) \to \gamma\gamma] = \hat{\mathbf{k}}_1 \cdot \boldsymbol{\varepsilon}_1^* \times \boldsymbol{\varepsilon}_2^* \, \mathbb{A}_{\mathrm{NRQCD}}, \tag{7a}$$

$$\mathbb{A}_{\mathrm{NRQCD}} = c_0 \langle 0|\chi^\dagger \psi |Q\overline{Q}(^1S_0^{[1]})\rangle + \frac{c_2}{m^2}\langle 0|\chi^\dagger(-\tfrac{i}{2}\overleftrightarrow{\mathbf{D}})^2\psi|Q\overline{Q}(^1S_0^{[1]})\rangle + \cdots . \tag{7b}$$

In Eq. (7), we again adopt the nonrelativistic normalization for the Q and $\overline{Q}$ states in the computations of the full QCD amplitude and the NRQCD matrix elements.

One can organize the full amplitude $\mathcal{A}$ in powers of the relative momentum between Q and $\overline{Q}$, denoted by $\mathbf{q}$:

$$\mathcal{A}[Q\overline{Q}(^1S_0^{[1]}) \to \gamma\gamma] = \hat{\mathbf{k}}_1 \cdot \boldsymbol{\varepsilon}_1^* \times \boldsymbol{\varepsilon}_2^* \left[\mathscr{A}_0 + \frac{\mathbf{q}^2}{m^2}\mathscr{A}_2 + \mathcal{O}(\mathbf{q}^4)\right]. \tag{8}$$

For convenience, we have again factored out the kinematic invariant $\hat{\mathbf{k}}_1 \cdot \boldsymbol{\varepsilon}_1^* \times \boldsymbol{\varepsilon}_2^*$ in the amplitude. To the desired accuracy, one can truncate the series at $\mathcal{O}(\mathbf{q}^2)$, with the first two Taylor coefficients denoted by $\mathscr{A}_0$ and $\mathscr{A}_2$. To our purpose, we need compute both $\mathscr{A}_i$ through NLO in α_s. This will be conducted in Section IV.

The NRQCD amplitude $\mathbb{A}_{\rm NRQCD}$ in (7), or equivalently, the NRQCD vacuum-to-$Q\overline{Q}$ matrix elements, need also be worked out in perturbation theory through $\mathcal{O}(\alpha_s)$. The encountered NRQCD matrix elements at LO in α_s are particularly simple [2]:

$$\langle 0|\chi^\dagger\psi|Q\overline{Q}({}^1S_0^{[1]})\rangle^{(0)} = \sqrt{2N_c}, \tag{9a}$$

$$\langle 0|\chi^\dagger(-\frac{i}{2}\overleftrightarrow{\mathbf{D}})^2\psi|Q\overline{Q}({}^1S_0^{[1]})\rangle^{(0)} = \sqrt{2N_c}\,\mathbf{q}^2, \tag{9b}$$

where the factor $\sqrt{2N_c}$ is due to the spin and color factors of the normalized $Q\overline{Q}({}^1S_0^{[1]})$ state. The computation of these matrix elements to $\mathcal{O}(\alpha_s)$ will be addressed in Section V.

III. TECHNIQUES ABOUT COMPUTING FULL QCD AMPLITUDE

In this section, we outline some necessary techniques about calculating the amplitude for $Q\overline{Q}({}^1S_0^{[1]}) \to \gamma\gamma$.

A. Kinematic setup

Let p and $\bar{p}$ represent the momenta carried by Q and $\overline{Q}$, respectively. It is customary to decompose them in the following form:

$$p = \frac{1}{2}P + q, \tag{10a}$$

$$\bar{p} = \frac{1}{2}P - q, \tag{10b}$$

where P is the total momentum of the $Q\overline{Q}({}^1S_0^{[1]})$ pair with invariant mass $\sqrt{P^2} = 2E$, q is the relative momentum. Enforcing Q and $\overline{Q}$ to stay on their mass shells, one requires that $E = \sqrt{m^2 - q^2}$ and $P \cdot q = 0$.

In the rest frame of the $Q\overline{Q}$ pair, which is our default choice, the explicit forms of all the momenta are given by

$$P^\mu = (2E, 0), \tag{11a}$$

$$q^\mu = (0, \mathbf{q}), \tag{11b}$$

$$p^\mu = (E, \mathbf{q}), \tag{11c}$$

$$\bar{p}^\mu = (E, -\mathbf{q}). \tag{11d}$$

[2] Unless otherwise stated, throughout this work we use the superscripts (0) and (1) to indicate the LO and NLO contributions in α_s, and the subscripts 0 and 2 to represent the LO and NLO contributions in v^2.

Hence the total momentum P becomes purely timelike, while the relative momentum q is purely spacelike, and one has $q^2 = -\mathbf{q}^2$ and $E = \sqrt{m^2 + \mathbf{q}^2}$. In this frame, the momenta carried by both photons have a magnitude of E.

For latter use, we define two velocity variables:

$$\beta \equiv \frac{|\mathbf{q}|}{E}, \tag{12a}$$

$$v \equiv \frac{|\mathbf{q}|}{m}. \tag{12b}$$

We will distinguish these two variables even in the nonrelativistic limit.

B. Covariant projection approach

1. *Projection of spin-singlet $Q\overline{Q}$ state*

We start with the quark amplitude $Q(p)\overline{Q}(\bar{p}) \to \gamma(k_1, \varepsilon_1) + \gamma(k_2, \varepsilon_2)$, with the momenta of Q and $\overline{Q}$ defined in (10):

$$\bar{u}(p) T v(\bar{p}) = \mathrm{Tr}\big[v(\bar{p})\bar{u}(p)T\big]. \tag{13}$$

Here T denotes a matrix in Dirac-color space.

To proceed, we need first to project the amplitude (13) onto the spin-singlet color-singlet $Q(p)\overline{Q}(\bar{p})$ state, by replacing the $v(\bar{p})\bar{u}(p)$ with a suitable projection matrix. The projector that is valid to all orders in $\mathbf{q}$ for the spin-singlet color-singlet channel, denoted by $\Pi_1^{(1)}(p, \bar{p})$, was first derived in [9]:

$$\begin{aligned}
\Pi_1^{(1)}(p, \bar{p}) &= \sum_{s_1, s_2} u(p, s_1)\bar{v}(\bar{p}, s_2)\langle \frac{1}{2}, s_1; \frac{1}{2}, s_2 | 00\rangle \otimes \frac{\mathbf{1}_c}{\sqrt{N_c}} \\
&= \frac{1}{8\sqrt{2}E^2(E+m)}(\not{p} + m)(\not{P} + 2E)\,\gamma_5(\not{\bar{p}} - m) \otimes \frac{\mathbf{1}_c}{\sqrt{N_c}},
\end{aligned} \tag{14}$$

where $\mathbf{1}_c$ is the unit matrix in the fundamental representation of the color $SU(3)$ group. The above spin-singlet projector is derived by assuming the nonrelativistic normalization convention for Dirac spinor. Applying this projector to (13), one obtains the amplitude for a spin/color-singlet $Q\overline{Q}$ pair annihilation decay into two photons:

$$\mathcal{A}^{\mathrm{sing}}[Q\overline{Q} \to \gamma\gamma] = \mathrm{Tr}\Big\{\Pi_1^{(1)}(p, \bar{p})T\Big\}, \tag{15}$$

where the trace is understood to act on both Dirac and color spaces.

2. Projection of S-wave amplitude

In the amplitude in (15), the $Q\overline{Q}$ pair is warranted to be in the spin-singlet state, but not necessarily in the S-wave orbital-angular-momentum state. To project out the S-wave amplitude, one needs average the amplitude $\mathcal{A}^{\rm sing}$ over all the directions of the relative momentum $\mathbf{q}$ in the $Q\overline{Q}$ rest frame. Afterwards one expands the resulting S-wave amplitude in powers of $\mathbf{q}^2$ and truncate the series at the desired order.

A question may concern us immediately– should the relative momentum q be taken as a 4-dimensional or a D-dimensional vector upon S-wave angular averaging? Since for our process the matching can be conducted solely at amplitude level, there is no *a priori* criterion to tell which treatment is superior. At first glancing, our incapability to pick up a "unique" and "correct" scheme may look troublesome, since different treatments may, conceivably, lead to different answers for the full QCD amplitude once beyond LO in $\mathbf{q}^2$ expansion. Nevertheless, it is possible that both schemes are equally acceptable, provided that ultimately they yield *identical* short-distance coefficients. In this respect, the ambiguity about the dimensionality of q may turn into a virtue, in that it can serve as a useful consistency check against our calculation. In Section IV, we will separately treat q^μ to be 4-dimensional (dubbed q_4 scheme), and D-dimensional (labeled q_D scheme) [3].

Since we are only concerned with the first-order relativistic correction, we will follow a standard shortcut to extract the S-wave amplitude rather than literally perform the angular integration. In q_4 scheme, we first expand the spin-singlet amplitude $\mathcal{A}^{\rm sing}$ in q^μ through the quadratic order, then make the following replacement:

$$q^\mu q^\nu \;\to\; \frac{\mathbf{q}^2}{3}\,\Pi^{\mu\nu}(P) \qquad\qquad (q_4 \text{ scheme}), \tag{16}$$

where

$$\Pi^{\mu\nu}(P) \;\equiv\; -g^{\mu\nu} + \frac{P^\mu P^\nu}{P^2}.$$

Subsequently we would be able to identify $\mathscr{A}_i$ $(i = 0, 2)$ as indicated in (8).

[3] Since $q^0 = 0$ in the rest frame of the $Q\overline{Q}$ pair, it seems more natural to view q^μ as either a 3-dimensional or a $D-1$-dimensional vector. Nevertheless, in the lack of confusion, we will stick to the terms q_4 and q_D scheme.

If q^μ is assumed to be a D-dimensional Lorentz vector, one can follow the same step as described above, except one make the following substitution:

$$q^\mu q^\nu \ \to \ \frac{\mathbf{q}^2}{D-1}\,\Pi^{\mu\nu}(P) \qquad\qquad (q_D \text{ scheme}). \tag{17}$$

We stress that in both schemes, the momenta P, k_1, k_2 and polarization vectors ε_1, ε_2 are always assumed to reside only in physical spacetime dimensions.

C. γ_5-prescription in Dimensional Regularization

When applying the covariant spin-singlet projector as given in Sec. III B 1, one needs to deal with the trace of γ_5 with a string of Dirac γ-matrices. This will pose one notorious problem, that a definite prescription of γ_5 must be specified if the spacetime dimension D is deformed from four.

We first point out that, for our process, in principle there exists no any technical subtlety about γ_5 in the q_4 scheme. One can always choose to first calculate the quark amplitude $Q\overline{Q} \to \gamma\gamma$ through NLO in α_s. As usual, dimensional regularization (DR) can be chosen to regularize both ultraviolet (UV) and infrared (IR) divergences. After the loop integration is done, one will end up with the T-matrix in (13) that only depends on the external kinematic variables, *e.g.* the momenta of quarks and photons, as well as the polarization vectors of photons, which are all 4-dimensional objects. Upon projecting out the spin-singlet amplitude, it is obviously legitimate to use the standard 4-dimensional trace formula involving γ_5 in (15).

In the q_D scheme, the γ_5 problem cannot be circumvented even if one first carries out the loop integration for the quark amplitude, because the quark momenta p and $\bar{p}$ appearing in the spin-singlet projector (14) can now penetrate into unphysical dimensions. In this case, the rule about D-dimensional trace operation involving γ_5 in (15) must be specified.

In practical computation, it is simpler to apply (15) prior to carrying out the loop integration. Since the internal fermion propagators and vertices are all D-dimensional objects, and all of them will enter into the trace, it becomes compulsory to specify the prescription of γ_5 in DR, for both q_D and q_4 schemes.

In literature, there are two popular prescriptions about γ_5 in DR, the naive dimensional regularization (NDR) [25, 26] and 't Hooft-Veltman dimensional regularization (HVDR) [27,

28]. In the former prescription, one assumes $\{\gamma_5, \gamma^\mu\} = 0$ for all $\mu = 0, 1, \cdots, D-1$. In the latter, one explicitly constructs $\gamma_5 \equiv i\gamma^0\gamma^1\gamma^2\gamma^3$, which anticommutes with γ^μ for $\mu = 0, 1, 2, 3$ but commutes with γ^μ for $\mu = 4, \cdots, D-1$.

In an arbitrary dimension, the definition $\mathrm{Tr}[\gamma_5\gamma^\mu\gamma^\nu\gamma^\alpha\gamma^\beta] = -4i\epsilon^{\mu\nu\alpha\beta}$ and $\{\gamma_5, \gamma^\mu\} = 0$ are incompatible [28], therefore γ_5 in NDR is an ambiguous object. In order to obtain consistent predictions in this scheme, one must impose some additional rules, *e.g.*, to give up the cyclicity property of trace and to place γ_5 in a fixed position called "reading point" [26]. Nevertheless, for its technical simplicity, the NDR scheme has been widely utilized in computing the NLO QCD corrections to quarkonium decay and production processes [29], though most of which are at the LO accuracy in v only [4].

In contrast to NDR, the HVDR scheme turns to be a mathematically consistent scheme, in which γ_5 is a well-defined and unique object. For example, the HVDR scheme can automatically guarantee to recover the celebrated Adler-Bell-Jackiw chiral anomaly, while in the NDR scheme, some *ad hoc* prescription has to be imposed to achieve this.

In HVDR, the γ-matrices in D dimension obey the following anticommutation algebra:

$$\{\gamma^\mu, \gamma^\nu\} \;=\; 2g^{\mu\nu}, \qquad \{\gamma_5, \gamma^\mu\} = 2\hat{g}^\mu_\nu\gamma_5\gamma^\nu. \tag{18}$$

$\hat{g}_{\mu\nu}$ denotes the projection of the metric tensor onto the unphysical dimensions, which equals $g_{\mu\nu}$ for $\mu, \nu = 4, \cdots, D-1$, and equals 0 otherwise. Some useful relations about this tensor are $\hat{g}^\mu_\mu = D-4$, $\hat{g}_{\mu\alpha}\hat{g}^\alpha_\nu = \hat{g}_{\mu\alpha}g^\alpha_\nu = \hat{g}_{\mu\nu}$. A nuisance of the HVDR scheme is that, since the first four dimensions are singled out as special, Lorentz covariance has been sacrificed in the intermediate stage. Moreover, one may get the impression that the messy anticommutation rule for γ_5 in D dimension would render the practical calculation a formidable task.

In this work, in favor of its internal consistency, we choose to work with the HVDR scheme. It is necessary to spell out the recipe of D-dimensional trace operation involving γ_5 in this scheme. In arbitrary spacetime dimension, the trace of a γ_5 with odd number of γ-matrices always vanishes. Starting from (18), West has derived a recursive formula for the

[4] It has also been pointed out in [29], that the γ_5-prescription implicit in the threshold expansion technique developed by Braaten and Chen [30, 31] is essentially equivalent to NDR.

trace of γ_5 with an even number of γ-matrices [32]:

$$\mathrm{Tr}[\gamma_5\gamma^{\mu_1}\gamma^{\mu_2}\gamma^{\mu_3}\gamma^{\mu_4}] = -4i\,\epsilon^{\mu_1\mu_2\mu_3\mu_4}, \tag{19a}$$

$$\mathrm{Tr}[\gamma_5\gamma^{\mu_1}\gamma^{\mu_2}\cdots\gamma^{\mu_n}] = \frac{2}{n-4}\sum_{i=2}^{n}\sum_{j=1}^{i-1}(-1)^{i+j+1}g^{\mu_i\mu_j}\mathrm{Tr}\left[\gamma_5\prod_{k=1(\neq i,j)}^{n}\gamma^{\mu_k}\right] \quad (\text{for } n\geq 6), \tag{19b}$$

where the Levi-Civita tensor is a 4-dimensional object in HVDR, *i.e.*, $\hat{g}^{\mu}_{\alpha}\epsilon_{\mu\nu\beta\gamma} = 0$.

One attractive point of West's trace formula is that, it involves only the 4-dimensional antisymmetric tensor together with the D-dimensional metric tensor (not the evanescent metric tensor $\hat{g}_{\mu\nu}$!). As a consequence, this recursive algorithm can be readily implemented in the MATHEMATICA packages specialized to high energy physics, such as FEYNCALC [33].

Equation (19) is valid in any dimension, of course also in $D = 4$, however it is superficially much more involved than the familiar 4-dimensional trace formula [5].

To make use of West's formula when projecting out the spin-singlet amplitude, we can employ the cyclicity of trace to move γ_5 in (15) to the leftmost, since this property persists to be a valid operation in the HVDR scheme:

$$\mathcal{A}^{\mathrm{sing}}(Q\overline{Q}\to\gamma\gamma) = \frac{1}{8\sqrt{2N_c}E^2(E+m)}\mathrm{Tr}\Big\{\gamma_5(\not{p}-m)T\,(\not{p}+m)(\not{P}+2E)\Big\}, \tag{20}$$

and the color trace has been implicit.

For obvious reason, we would not bother to use the anti-commutation relation of γ_5 to realize this goal.

IV. QCD AMPLITUDE OF $Q\overline{Q}(^1S_0^{[1]}) \to \gamma\gamma$ THROUGH NLO IN α_s

In this section we employ the covariant projection technique described in the preceding section to compute $Q\overline{Q}(^1S_0^{[1]}) \to \gamma\gamma$ through NLO in α_s. The HVDR scheme will be used throughout.

[5] For example, in the HVDR scheme, the trace of γ_5 with six γ-matrices will result in 15 terms, in contrast to the 6 terms that one would directly obtain in 4 dimension.

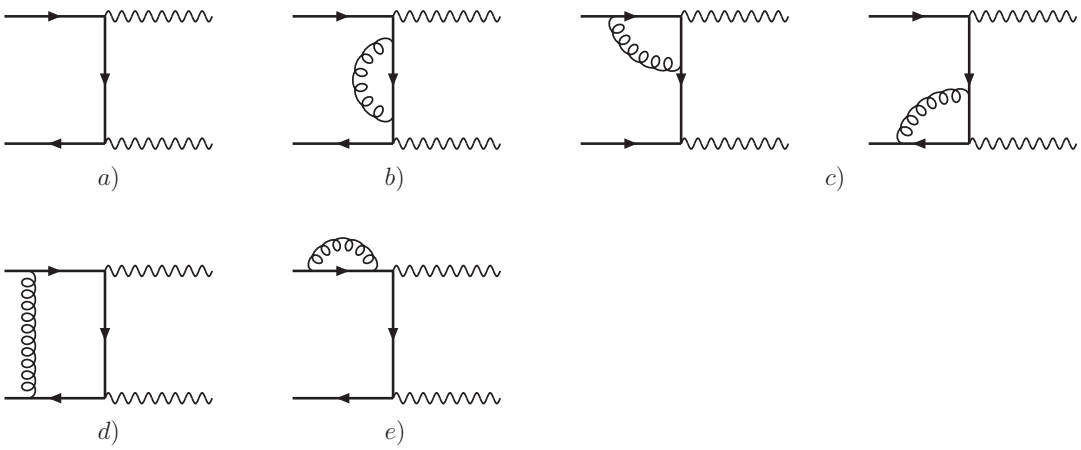


FIG. 1: Feynman diagrams for $Q\overline{Q}(^1S_0^{[1]}) \to \gamma\gamma$ through $\mathcal{O}(\alpha_s)$. For simplicity, the crossed diagrams have been suppressed.

A. Tree-level amplitude and matching coefficients

There are two $\mathcal{O}(\alpha_s^0)$ diagrams for $Q\overline{Q} \to \gamma\gamma$, one of which is illustrated in Fig. 1a). The corresponding LO T-matrix reads:

$$T^{(0)} \;=\; -ie^2e_Q^2\left[\not{\varepsilon}_2^*\frac{\not{p}-\not{k}_1+m}{-2p\cdot k_1}\not{\varepsilon}_1^*+\not{\varepsilon}_1^*\frac{-\not{\bar{p}}+\not{k}_1+m}{-2\bar{p}\cdot k_1}\not{\varepsilon}_2^*\right]\otimes\mathbf{1}_c. \tag{21}$$

If q lives only in physical dimensions, one can directly substitute (21) into (15) to project out the spin-singlet amplitude, and use the 4-dimensional trace formula to obtain [9]:

$$\mathcal{A}^{\mathrm{sing}(0)}(Q\overline{Q}\to\gamma\gamma) \;=\; e^2e_Q^2\sqrt{2N_c}\,\hat{\mathbf{k}}_1\cdot\boldsymbol{\varepsilon}_1^*\times\boldsymbol{\varepsilon}_2^*\frac{mE^2}{E^4-(k_1\cdot q)^2}. \tag{22}$$

If q is instead allowed to leak into the unphysical dimensions, one needs substitute (21) into (20), and utilize (19) to carry out the D-dimensional trace:

$$\begin{aligned}\mathcal{A}^{\mathrm{sing}(0)}(Q\overline{Q}\to\gamma\gamma) &= e^2e_Q^2\sqrt{\frac{N_c}{2}}\frac{1}{(E+m)(E^4-(k_1\cdot q)^2)}\\ \times\;&\left[E(E+m)\epsilon^{\mu\nu\alpha\beta}k_{1\alpha}+\epsilon^{\mu\alpha\beta\gamma}k_{1\alpha}q_\gamma q^\nu-\epsilon^{\nu\alpha\beta\gamma}k_{1\alpha}q_\gamma q^\mu+\epsilon^{\mu\nu\alpha\beta}q_\alpha k_1\cdot q\right]P_\beta\varepsilon_{1\mu}^*\varepsilon_{2\nu}^*.\end{aligned} \tag{23}$$

We have dropped those terms linear in q, which trivially vanish due to the constraints $P\cdot\varepsilon_i=0$ and $P^0=2k_1^0$. Note this expression is much more complicated than (22), though they should be exactly identical when q is a 4-dimensional vector.

The Levi-Civita tensor, k_1, ε_1 and ε_2 are all 4-dimensional quantities. For any q vector in (23) that contracts with them, only its first four components can contribute, that is, one can

make the replacement $q^\alpha \to \bar{q}^\alpha \equiv (g^\alpha_\beta - \hat{g}^\alpha_\beta)q_\beta$, without affecting the answer. The unphysical components of q, $\hat{q}^\alpha \equiv \hat{g}^\alpha_\beta q_\beta$, contribute to (23) only implicitly through the factor E.

Expand (22) and (23) in q, then apply (16) and (17), one can pick up the corresponding tree-level S-wave amplitudes in the q_4 and q_D schemes. It is then straightforward to identify $\mathscr{A}_i^{(0)}$ as introduced in (8):

$$\mathscr{A}_0^{(0)} = \sqrt{2N_c}\,\frac{4\pi e_Q^2\alpha}{m}, \tag{24a}$$

$$\mathscr{A}_2^{(0)}\bigg|_{q_4 \text{ scheme}} = -\sqrt{2N_c}\,\frac{8\pi e_Q^2\alpha}{3m}, \tag{24b}$$

$$\mathscr{A}_2^{(0)}\bigg|_{q_D \text{ scheme}} = -\sqrt{2N_c}\,\frac{2D\pi e_Q^2\alpha}{(D-1)m}. \tag{24c}$$

Not surprisingly, the $\mathcal{O}(v^2)$ S-wave amplitudes differ in q_4 and q_D schemes.

The NRQCD matarix elements at LO in α_s have been given in (9). According to (7b), one can write down the Born-order perturbative NRQCD amplitude:

$$\mathbb{A}^{(0)}_{\text{NRQCD}} = \sqrt{2N_c}\left[c_0^{(0)} + c_2^{(0)}v^2 + \cdots\right]. \tag{25}$$

Combining (7), (8), (24) and (25), one easily recognizes the $\mathcal{O}(\alpha_s^0)$ short-distance coefficients $c_i^{(0)} = \mathscr{A}_i^{(0)}/\sqrt{2N_c}$ $(i = 0, 2)$:

$$c_0^{(0)} = \frac{4\pi e_Q^2\alpha}{m}, \tag{26a}$$

$$c_2^{(0)}\bigg|_{q_4 \text{ scheme}} = -\frac{8\pi e_Q^2\alpha}{3m}, \tag{26b}$$

$$c_2^{(0)}\bigg|_{q_D \text{ scheme}} = -\frac{2-\epsilon}{3-2\epsilon}\frac{4\pi e_Q^2\alpha}{m}, \tag{26c}$$

where as usual, $D \equiv 4 - 2\epsilon$. The coefficient $c_2^{(0)}$ in q_D scheme differs from that in q_4 scheme by an $\mathcal{O}(\epsilon)$ constant. At first sight, it seems no need to retain this extra piece since no any divergence emerges at this order. However, as will become clear later, this $\mathcal{O}(\epsilon)$ piece plays a key role for ultimately obtaining the scheme-independent $\mathcal{O}(\alpha_s)$ short-distance coefficients.

B. QCD amplitude at NLO in α_s

We proceed to compute NLO QCD correction to the $Q\overline{Q}(^1S_0^{[1]}) \to \gamma\gamma$ process. At $\mathcal{O}(\alpha_s)$, there are eight one-loop diagrams, including two self-energy diagrams, four triangle diagrams and two box diagrams. Half of these diagrams have been shown in Fig. 1*b*) through 1*d*).

Each individual NLO diagram may contain UV or IR divergences. For example, the self-energy and triangle diagrams contain UV divergences, and the box diagrams possess IR divergence. We will choose DR as a convenient regulator to regularize both types of divergences. Since our concern is to calculate the gauge-invariant on-shell amplitude, for simplicity we will work with Feynman gauge in this Section.

In accordance with the LSZ reduction formula, we need multiply the tree-level amplitude in Fig. 1a) by the residue of the heavy quark propagator at its pole, Z_Q. This contribution is represented by Fig. 1e). In Feynman gauge, the residue is given by

$$Z_Q \;=\; 1 - \frac{C_F \alpha_s}{4\pi} \left(\frac{1}{\epsilon_{\rm UV}} + \frac{2}{\epsilon_{\rm IR}} - 3\gamma_E + 3 \ln \frac{4\pi\mu^2}{m^2} + 4 \right) + \mathcal{O}(\alpha_s^2), \tag{27}$$

where γ_E is the Euler constant, and $C_F = \frac{N_c^2-1}{2N_C}$ is the Casmir for the fundamental representation of the $SU(N_c)$ group.

In addition, we also need replace the bare quark mass in the quark propagator in Fig. 1a) by

$$m^{\rm bare} \;=\; m \left[1 - \frac{C_F \alpha_s}{4\pi} \left(\frac{3}{\epsilon_{\rm UV}} - 3\gamma_E + 3 \ln \frac{4\pi\mu^2}{m^2} + 4 \right) + \mathcal{O}(\alpha_s^2) \right]. \tag{28}$$

It is straightforward to write down the respective $T^{(1)}$-matrix for each NLO diagram in Fig. 1. We then substitute them into (20), and for simplicity, use (19) to carry out the D-dimensional trace prior to performing loop integration [6].

Practically, we resort to the MATHEMATICA package FEYNCALC [33] to accomplish the abovementioned trace operation, because West's formula (19) is its built-in algorithm for calculating the trace involving γ_5. We continue to use FEYNCALC to reduce all the encountered one-loop tensor integrals to the one-loop scalar integrals. It turns out that only a couple of two-point, three-point scalar integrals and one four-point scalar integral are required. For reader's convenience, the closed-form expressions for these scalar integrals have been collected in Appendix A.

By far we have obtained the analytic expression for $\mathcal{A}^{\rm sing(1)}$, the $\mathcal{O}(\alpha_s)$ spin-singlet amplitude for $Q\overline{Q} \to \gamma\gamma$. We proceed to expand it to second order in q, then apply (16) and (17) to extract the corresponding S-wave amplitudes defined in (8), in both q_4 and q_D schemes,

[6] Since γ_5 in the HVDR scheme is mathematically unambiguous, reversing the order of trace and loop integration would not affect the final result.

TABLE I: The individual contributions to the $Q\overline{Q}(^1S_0^{[1]}) \to 2\gamma$ amplitude, $\mathscr{A}_0$ and $\mathscr{A}_2$, from different classes of diagrams in Fig. 1. A common factor $\sqrt{2N_c}\left(\frac{4\pi e_Q^2\alpha}{m}\right)$ has been suppressed for the Born-order results, while a common factor $\sqrt{2N_c}\left(\frac{4C_F e_Q^2\alpha\alpha_s}{m}\right)$ has also been dropped for the $\mathcal{O}(\alpha_s)$ results. For brevity, we have used the shorthand $\frac{1}{\hat{\epsilon}} \equiv \frac{1}{\epsilon} - \gamma_E + \ln\frac{4\pi\mu^2}{m^2}$.

QCD diagrams	q_4 scheme	q_D scheme
	$\mathscr{A}_0$	
$1a)$	1	
$1b)$	$-\frac{1}{\hat{\epsilon}_{\rm UV}} + 2\ln 2 - \frac{3}{2}$	
$1c)$	$\frac{1}{2}\frac{1}{\hat{\epsilon}_{\rm UV}} - 2\ln 2 + \frac{\pi^2}{8}$	
$1d)$	$\frac{\pi^2}{4v} + \frac{i\,\pi}{4v}\left(-\frac{1}{\hat{\epsilon}_{\rm IR}} + 2\ln(2v)\right) + \frac{1}{2}\frac{1}{\hat{\epsilon}_{\rm IR}} - 1$	
$1e)$	$\frac{1}{2}\left(\frac{1}{\hat{\epsilon}_{\rm UV}} - \frac{1}{\hat{\epsilon}_{\rm IR}}\right)$	
	$\mathscr{A}_2$	
$1a)$	$-\frac{2}{3}$	$-\frac{2}{3} - \frac{\epsilon}{9}$
$1b)$	$\frac{7}{6}\frac{1}{\hat{\epsilon}_{\rm UV}} - \frac{8}{3}\ln 2 + \frac{7}{3}$	$\frac{7}{6}\frac{1}{\hat{\epsilon}_{\rm UV}} - \frac{8}{3}\ln 2 + \frac{41}{18}$
$1c)$	$-\frac{1}{3}\frac{1}{\hat{\epsilon}_{\rm UV}} + \frac{10}{3}\ln 2 - \frac{\pi^2}{8} - \frac{1}{6}$	$-\frac{1}{3}\frac{1}{\hat{\epsilon}_{\rm UV}} + \frac{10}{3}\ln 2 - \frac{\pi^2}{8} - \frac{2}{9}$
$1d)$	$\frac{5\pi^2}{24v} + \frac{5i\,\pi}{24v}\left(-\frac{1}{\hat{\epsilon}_{\rm IR}} + 2\ln(2v)\right)$	$\frac{5\pi^2}{24v} + \frac{5i\,\pi}{24v}\left(-\frac{1}{\hat{\epsilon}_{\rm IR}} + 2\ln(2v) + \frac{2}{15}\right)$
	$+\frac{1}{3}\frac{1}{\hat{\epsilon}_{\rm IR}} - 2\ln 2 - \frac{4}{9}$	$+\frac{1}{3}\frac{1}{\hat{\epsilon}_{\rm IR}} - 2\ln 2 - \frac{1}{2}$
$1e)$	$-\frac{5}{6}\frac{1}{\hat{\epsilon}_{\rm UV}} + \frac{1}{3}\frac{1}{\hat{\epsilon}_{\rm IR}} - \frac{2}{3}$	$-\frac{5}{6}\frac{1}{\hat{\epsilon}_{\rm UV}} + \frac{1}{3}\frac{1}{\hat{\epsilon}_{\rm IR}} - \frac{1}{2}$

respectively. The intermediate steps are straightforward but cumbersome, and some special care has to be paid when dealing with the box diagrams. Fortunately, almost all these manipulations can be handled by computer.

For completeness and for clarity, we tabulate in Table. I the individual contributions to the S-wave amplitudes $\mathscr{A}_0^{(1)}$ and $\mathscr{A}_2^{(1)}$ from each class of diagrams, in both q_4 and q_D schemes. For each entry, we sum all the diagrams that belong to the same topology class, including the crossed ones. The entry "$1e$)" in Table I refers to the $\mathcal{O}(\alpha_s)$ contributions from both wave function and mass renormalization, as specified in (27) and (28).

As can be seen from Table I, the Coulomb singularity arises in the box diagrams, present in both $\mathscr{A}_0^{(1)}$ and $\mathscr{A}_2^{(1)}$. The emergence of this π^2/v singularity reflects that the real part can receive the contribution from the *potential* region. For completeness, we also explicitly

include the contributions of the imaginary part from the box diagrams. This corresponds to a configuration that the two non-adjacent Q and $\overline{Q}$ quarks in the box can become simultaneously on their mass-shells, so that the exchanged gluon can only be *potential* mode. Consequently, only the potential region can contribute to the imaginary part, which is plagued with the joint $i\pi/v$ and IR singularities as well as the term nonanalytic in $\mathbf{q}$. We expect that the corresponding $\mathcal{O}(\alpha_s)$ NRQCD calculation in next section will exactly reproduce such potential-region contributions.

Another observation from Table. I is that, both the q_4 and q_D schemes differ on the $\mathcal{O}(v^2)$ contributions in each individual diagram. This pattern is in sharp contrast to the $\mathcal{O}(v^0)$ case.

Summing up all the individual contributions listed in Table. I, one finally obtains the complete NLO QCD amplitude for $Q\overline{Q}(^1S_0^{[1]}) \to \gamma\gamma$:

$$\mathscr{A}_0^{(1)} = \sqrt{2N_c}\,\frac{4C_F e_Q^2 \alpha\alpha_s}{m}\left[\frac{\pi^2-20}{8}+\frac{\pi^2}{4v}+\frac{i\,\pi}{4v}\left(-\frac{1}{\epsilon_{\rm IR}}+\gamma_E+\ln\frac{\mathbf{q}^2}{\pi\mu^2}\right)\right], \tag{29a}$$

$$\begin{aligned}\mathscr{A}_2^{(1)} = \sqrt{2N_c}\,\frac{4C_F e_Q^2 \alpha\alpha_s}{m}\Bigg[&\frac{2}{3}\left(\frac{1}{\epsilon_{\rm IR}}-\gamma_E+\ln\frac{4\pi\mu^2}{m^2}\right)+\frac{19}{18}-\frac{\pi^2}{8}-\frac{4}{3}\ln 2\\ &+\frac{5\pi^2}{24v}+\frac{5i\,\pi}{24v}\left(-\frac{1}{\epsilon_{\rm IR}}+\gamma_E+\ln\frac{\mathbf{q}^2}{\pi\mu^2}\right)+C_q\Bigg].\end{aligned} \tag{29b}$$

Interestingly, both the q_4 and q_D schemes now fully agree on the real part of the complete $\mathcal{O}(v^2)$ amplitude, and only differ slightly on the imaginary part. The scheme dependence is encoded in C_q, an imaginary constant, which equals 0 in q_4 scheme, and equals $\frac{i\pi}{36v}$ in q_D scheme. As will be seen in Sec. VI, the scheme-dependence of C_q is intimately correlated with that of $c_2^{(0)}$ in (26).

We make some further comments on the complete NLO QCD amplitude in (29). The UV divergences have been swept through the wave function and mass renormalization. At LO in v^2, the IR divergences in the real part completely cancel when summing up all diagrams, which is warranted by the neutral color charge of the S-wave $Q\overline{Q}$ pair [5]. Nevertheless, this cancelation fails to hold at NLO in v^2, and the presence of a net infrared divergence in the real part of (29b) signals that the simple "color-transparency" picture no longer applies, and the soft gluons can resolve the geometric details of the $Q\overline{Q}$ pair and may even strongly interact with its color dipole. It is easy to find that this IR divergence arises from the *soft* region of the loop diagrams. We anticipate that the corresponding $\mathcal{O}(\alpha_s)$ NRQCD calculation in next Section will exactly reproduce this infrared divergence at relative order v^2.

V. NRQCD AMPLITUDE AT NLO IN α_s

To match the accuracy of the QCD calculation for $Q\overline{Q}(^1S_0^{[1]}) \to \gamma\gamma$ in Section IV B, it is necessary to compute the perturbative NRQCD amplitude $\mathbb{A}_{\rm NRQCD}$ to NLO in α_s.

In (9), the two involved NRQCD matrix elements have been given at LO in α_s. In the following we proceed to compute their $\mathcal{O}(\alpha_s)$ corrections. For this purpose, the knowledge of the NRQCD lagrangian in the heavy quark bilinear sector is required [5]:

$$\begin{aligned}\mathcal{L}_{\rm NRQCD} &= \psi^\dagger\left(iD_0 + \frac{\mathbf{D}^2}{2m}\right)\psi + \psi^\dagger\frac{\mathbf{D}^4}{8m^3}\psi + \frac{c_F}{2m}\psi^\dagger\boldsymbol{\sigma}\cdot g_s\mathbf{B}\psi \\ &+ \frac{c_D}{8m^2}\psi^\dagger(\mathbf{D}\cdot g_s\mathbf{E} - g_s\mathbf{E}\cdot\mathbf{D})\psi + \frac{ic_S}{8m^2}\psi^\dagger\boldsymbol{\sigma}\cdot(\mathbf{D}\times g_s\mathbf{E} - g_s\mathbf{E}\times\mathbf{D})\psi \\ &+ \left(\psi \to i\sigma^2\chi^*, A_\mu \to -A_\mu^T\right) + \mathcal{L}_{\rm light}\,. \end{aligned} \tag{30}$$

The replacement in the last line implies that the corresponding heavy anti-quark bilinear sector can be obtained through the charge conjugation transformation. $\mathcal{L}_{\rm light}$ represents the lagrangian for the light quarks and gluons.

The short-distance coefficients c_F, c_D, c_S, in (30) are associated with the Fermi, Darwin, and spin-obit interactions, respectively. To our purpose, suffices it to know their tree-level values $c_F = c_D = c_S = 1 + \mathcal{O}(\alpha_s)$. Moreover, in (30) we have neglected all other higher-dimensional operators, since the relativistic corrections generated by them are beyond the intended $\mathcal{O}(v^2)$ accuracy.

Through the relative order v^2, the $\mathcal{O}(\alpha_s)$ corrections to the matrix elements stem from the one-loop NRQCD diagrams as illustrated in Fig. 2. The first six diagrams [7] represent the one-loop correction to the matrix element $\langle 0|\chi^\dagger\psi|Q\overline{Q}(^1S_0^{[1]})\rangle$, while the last one in Fig. 2 constitutes the one-loop correction to $\langle 0|\chi^\dagger(-\frac{i}{2}\overleftrightarrow{\mathbf{D}})^2\psi|Q\overline{Q}(^1S_0^{[1]})\rangle$.

In passing, we note that our one-loop correction calculation for the vacuum-to-$Q\overline{Q}(^1S_0)$ NRQCD matrix elements is quite similar to the existing one for the vacuum-to-$Q\overline{Q}(^3S_1)$ matrix elements [21]. Since heavy quark spin symmetry is violated at relative order v^2, we cannot completely transplant their results here. Ref. [21] uses Feynman gauge in calculating NRQCD diagrams. In contrast, in this section we will work in the Coulomb gauge, since it has the virtue that the instantaneous (potential) nature of the temporal gluon becomes

[7] We have not drawn the diagram in which a temporal gluon attaches to a spin-orbit interaction vertex and a Coulomb vertex, because its contribution simply vanishes due to spin conservation.

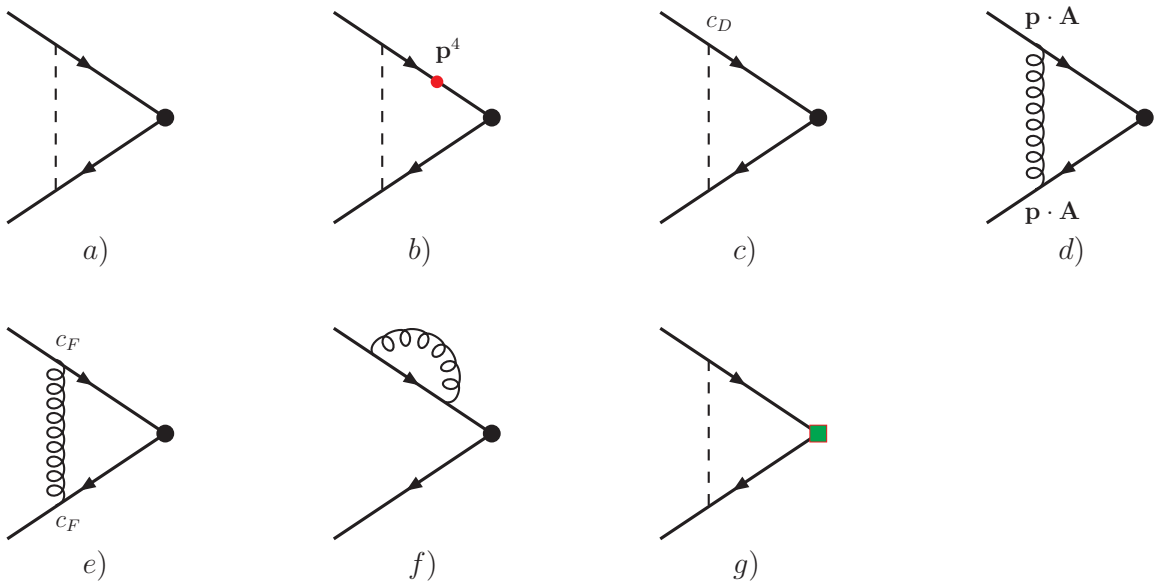


FIG. 2: The one-loop NRQCD diagrams that initiate the $\mathcal{O}(\alpha_s)$ corrections to the vacuum-to-$Q\overline{Q}(^1S_0^{[1]})$ matrix elements. The big solid circle represents the operator $\chi^\dagger\psi$, while the solid square represents the operator $\chi^\dagger(-\frac{i}{2}\overleftrightarrow{\mathbf{D}})^2\psi$. The dashed line denotes the temporal gluon, and the curly line denotes the transverse gluon. The unlabeled vertex attached to a temporal gluon stands for the Coulomb interaction $\mp ig_sT^a$. For simplicity, we have suppressed the conjugate diagrams of b) and c), in which the same operators are inserted on the antiquark line.

manifest. Of course, insofar as the on-shell matrix element is concerned, the choice of gauge is merely a matter of convenience.

When computing the loop diagrams in Fig. 2, we first integrate over the temporal component k^0 using contour integration, where k signifies the loop momentum carried by the gluon propagator. We then perform the remaining integration over $\mathbf{k}$ in $D-1$ spatial dimension. When the exchanged gluon is transverse, as exemplified by Fig. 2d), the situation is somewhat more complicated. Upon integrating over k^0, one would end up with two terms, one with the residue taken at the pole of the quark propagator, and the other with the residue taken at the pole of the gluon propagator. The denominators of each resulting term are in general inhomogeneous in powers of v. This problem was initially overcome in a heuristic way by expanding the integrand [5]. This recipe was later clarified and systemized in the *method of region* formalism [22] (see also [21]). In this context, the two terms after con-

TABLE II: The analytic expressions of each $\mathcal{O}(\alpha_s)$ NRQCD diagram in Fig. 2 (in Coulomb gauge). For simplicity, we have stripped off an overall factor of $\sqrt{2N_c}\frac{C_F\alpha_s}{\pi}$.

NRQCD diagrams	Expressions
$2a)$	$\frac{1}{4v}\left[\pi^2+i\pi\left(-\frac{1}{\epsilon_{\rm IR}}+\gamma_E+\ln\frac{\mathbf{q}^2}{\pi\mu^2}-\frac{v^2}{4}\right)\right]$
$2b)$	$\frac{v}{8}\left[\pi^2+i\pi\left(-\frac{1}{\epsilon_{\rm IR}}+\gamma_E+\ln\frac{\mathbf{q}^2}{\pi\mu^2}+\frac{1}{2}\right)\right]$
$2c)$	$-\frac{v}{4}(i\pi)$
$2d)$	$\frac{v}{4}\left[\pi^2+i\pi\left(-\frac{1}{\epsilon_{\rm IR}}+\gamma_E+\ln\frac{\mathbf{q}^2}{\pi\mu^2}-1\right)\right]-\frac{v^2}{3}\left(\frac{1}{\epsilon_{\rm UV}}-\frac{1}{\epsilon_{\rm IR}}\right)$
$2e)$	$\frac{v}{2}(i\pi)$
$2f)$	$-\frac{v^2}{3}\left(\frac{1}{\epsilon_{\rm UV}}-\frac{1}{\epsilon_{\rm IR}}\right)$
$2g)$	$m^2\frac{v}{4}\left[\pi^2+i\pi\left(-\frac{1}{\epsilon_{\rm IR}}+\gamma_E+\ln\frac{\mathbf{q}^2}{\pi\mu^2}\right)\right]$

tour integration can be identified with the potential and soft region, respectively. For each region, loop momentum has a definite power in v so that one can readily homogenize the integrand by expanding the denominator accordingly. After this is done, it then becomes a straightforward exercise to carry out the spatial integrations in DR.

According to the LSZ reduction formula, we need multiply the LO matrix element $\langle 0|\chi^\dagger\psi|Q\overline{Q}(^1S_0)\rangle^{(0)}$ by the residue of the heavy quark propagator in NRQCD near its pole, $Z_{\rm NRQCD}$. The $\mathcal{O}(\alpha_s)$ piece of this contribution is represented by Fig. $2f$). In Coulomb gauge, the residue in DR reads [8]

$$Z_{\rm NRQCD}(q)=1-\frac{C_F\alpha_s}{3\pi}v^2\left(\frac{1}{\epsilon_{\rm UV}}-\frac{1}{\epsilon_{\rm IR}}\right). \tag{31}$$

It is worth noting that, the simultaneous occurrences of UV pole and IR pole at $\mathcal{O}(v^2)$ can be traced to a logarithmically-divergent scaleless integral in the soft region.

For clarity, we list in Table II the separate contribution from each diagram in Fig. 2. In Fig. $2a$), we follow [21] to include an extra source of relativistic correction that arises form the nonrelativistic expansion of the kinematic energy of the external (anti)quark $\frac{\mathbf{q}^2}{2m}-\frac{\mathbf{q}^4}{8m^3}$. For the entries corresponding to Fig. $2b$) and c), we have also included the contributions from their conjugate diagrams. It is clear to see that, all the diagrams receive contributions from the potential region (odd powers of v). In addition, Fig. $2d$) and f) also receive

[8] The Coulomb-gauge residue has been given in Appendix B of [5], which depends on a hard momentum cutoff there. We have converted that cutoff-scheme expression to its counterpart in DR.

the nonvanishing contributions from the soft region (even powers of v), which result in a logarithmically divergent scaleless integral. Only $\mathbf{p}\cdot\mathbf{A}$ interaction can result in such a contribution.

Summing all the individual contributions in Table II, we obtain the $\mathcal{O}(\alpha_s)$ corrections to the perturbative NRQCD matrix elements:

$$\langle 0|\chi^\dagger\psi|Q\overline{Q}({}^1S_0^{[1]})\rangle^{(1)} = \sqrt{2N_c}\frac{C_F\alpha_s}{\pi}\left\{\frac{1}{4v}\left(1+\frac{3}{2}v^2\right)\left[\pi^2+i\pi\left(-\frac{1}{\epsilon_{\rm IR}}+\gamma_E+\ln\frac{\mathbf{q}^2}{\pi\mu^2}\right)\right]\right.$$
$$\left.-\frac{2v^2}{3}\left(\frac{1}{\epsilon_{\rm UV}}-\frac{1}{\epsilon_{\rm IR}}\right)\right\}, \tag{32a}$$

$$\langle 0|\chi^\dagger(-\frac{i}{2}\overleftrightarrow{\mathbf{D}})^2\psi|Q\overline{Q}({}^1S_0^{[1]})\rangle^{(1)} = \sqrt{2N_c}\frac{C_F\alpha_s}{\pi}m^2\left(\frac{v}{4}\right)\left[\pi^2+i\pi\left(-\frac{1}{\epsilon_{\rm IR}}+\gamma_E+\ln\frac{\mathbf{q}^2}{\pi\mu^2}\right)\right]. \tag{32b}$$

As is evident in (32a), the order-α_s correction to the matrix element $\langle 0|\chi^\dagger\psi|Q\overline{Q}({}^1S_0)\rangle$ is logarithmically UV divergent, which can be traced back to the $\mathbf{p}\cdot\mathbf{A}$ interactions in Fig. 2d) and f). Employing the $\overline{\rm MS}$ scheme to subtract the UV divergence, we then obtain the renormalized matrix element

$$\langle 0|\chi^\dagger\psi|Q\overline{Q}({}^1S_0^{[1]})\rangle^{(1)}_{\overline{\rm MS}} = \sqrt{2N_c}\frac{C_F\alpha_s}{\pi}\left\{\frac{1}{4v}\left(1+\frac{3}{2}v^2\right)\left[\pi^2+i\pi\left(-\frac{1}{\epsilon_{\rm IR}}+\gamma_E+\ln\frac{\mathbf{q}^2}{\pi\mu^2}\right)\right]\right.$$
$$\left.+\frac{2v^2}{3}\left(\frac{1}{\epsilon_{\rm IR}}-\gamma_E+\ln 4\pi\right)\right\}. \tag{33}$$

According to (7b), accurate up to the order $\alpha_s v^2$, we can express the perturbative NRQCD amplitude as

$$\mathbb{A}_{\rm NRQCD} = (c_0^{(0)}+c_0^{(1)})\langle 0|\chi^\dagger\psi|Q\overline{Q}({}^1S_0^{[1]})\rangle^{(0)} + c_0^{(0)}\langle 0|\chi^\dagger\psi|Q\overline{Q}({}^1S_0^{[1]})\rangle^{(1)}_{\overline{\rm MS}} \tag{34}$$
$$+\frac{c_2^{(0)}+c_2^{(1)}}{m^2}\langle 0|\chi^\dagger(-\tfrac{i}{2}\overleftrightarrow{\mathbf{D}})^2\psi|Q\overline{Q}({}^1S_0^{[1]})\rangle^{(0)} + \frac{c_2^{(0)}}{m^2}\langle 0|\chi^\dagger(-\tfrac{i}{2}\overleftrightarrow{\mathbf{D}})^2\psi|Q\overline{Q}({}^1S_0^{[1]})\rangle^{(1)} + \cdots,$$

with all the involved NRQCD matrix elements available now. It is anticipated that (34) will faithfully reproduce the infrared behavior of (29).

VI. MATCHING THE SHORT-DISTANCE COEFFICIENTS AT NLO IN α_s

In section IV A we have already conducted the perturbative matching at tree level, and determined the tree-level coefficients $c_i^{(0)}$ $(i=0,2)$ in (26). Substituting their explicit values

into (34), and subtracting the contribution of the tree-level NRQCD amplitude $\mathbb{A}^{(0)}_{\rm NRQCD}$, one finds that the NRQCD amplitude at $\mathcal{O}(\alpha_s)$ reads:

$$\begin{aligned}\mathbb{A}^{(1)}_{\rm NRQCD} \;=\; & \sqrt{2N_c}\Bigg\{c_0^{(1)} + c_2^{(1)}v^2 + \frac{4C_F e_Q^2\alpha\alpha_s}{m}\Bigg\{\frac{2v^2}{3}\left(\frac{1}{\epsilon_{\rm IR}} - \gamma_E + \ln 4\pi\right) \\ & + \frac{1}{4v}\left(1+\frac{5}{6}v^2\right)\left[\pi^2 + i\pi\left(-\frac{1}{\epsilon_{\rm IR}} + \gamma_E + \ln\frac{\mathbf{q}^2}{\pi\mu^2}\right)\right] + \widetilde{C}_q v^2\Bigg\}\Bigg\}. \end{aligned} \tag{35}$$

Here $\widetilde{C}_q$ is a scheme-dependent imaginary constant. The origin of this constant can be easily traced, which arises from the last term in (34), that is, the $O(\epsilon)$ piece in the tree-level coefficient $c_2^{(0)}$ multiplied by the imaginary infrared pole in the matrix element $\langle 0|\chi^\dagger(-\frac{i}{2}\overleftrightarrow{\mathbf{D}})^2\psi|Q\overline{Q}({}^1S_0^{[1]})\rangle^{(1)}$ in (32b).

Remarkably, $\widetilde{C}_q$ turns out to exactly equal the scheme-dependent constant C_q that appears in the NLO QCD amplitude $\mathscr{A}_2^{(1)}$ in (29b), which vanishes in q_4 scheme, but equals $\frac{i\pi}{36v}$ in q_D scheme. Clearly, the equality of these two constants is by no means a coincidence.

Following (7) and (8), one readily recognizes the matching condition at order α_s:

$$\mathscr{A}_0^{(1)} + \mathscr{A}_2^{(1)}v^2 = \mathbb{A}^{(1)}_{\rm NRQCD}. \tag{36}$$

Plugging the analytic expressions of $\mathscr{A}_i^{(1)}$ $(i = 0, 2)$, which are given in (29), and the expression of $\mathbb{A}^{(1)}_{\rm NRQCD}$, as given in (35), into this matching equation, one observes that the infrared and Coulomb singularities, together with the terms non-analytic in $|\mathbf{q}|$, exactly cancel from the both sides of (36). This is of course as expected, which is warranted by the general construction of the NRQCD effective theory.

It is a nontrivial check for the consistency of our calculation, that the imaginary parts, which receive the contribution solely from the potential region, indeed fully cancel in both sides of (36). In particular, it is remarkable that the scheme-dependent imaginary pieces also cancel in both q_4 and q_D schemes, thanks to the equality $\widetilde{C}_q = C_q$. This cancelation is crucial for one to obtain the scheme-independent short-distance coefficients [9].

[9] We have made a further test of the scheme-independence of the coefficient $c_2^{(1)}$. In the QCD-side calculation, we attempt to use the alternative version of the spin/color-singlet projector [34]:

$$\widehat{\Pi}_1^{(1)}(p,\bar{p}) = \frac{1}{4\sqrt{2}E^2}(\not{p}+m)\,\gamma_5(\not{\bar{p}}-m)\otimes\frac{\mathbf{1}_c}{\sqrt{N_c}},$$

which is equivalent to (14) only in $D = 4$. Following the same procedure as described in the text to extract the ${}^1S_0^{[1]}$ amplitude, we obtain identical results as in (29) except for the C_q term. As expected,

It is then straightforward to solve the order-α_s short-distance coefficients:

$$c_0^{(1)} = \frac{4\pi e_Q^2 \alpha}{m} \frac{C_F \alpha_s}{\pi} \left(\frac{\pi^2}{8} - \frac{5}{2} \right), \tag{37a}$$

$$c_2^{(1)} = \frac{8\pi e_Q^2 \alpha}{3m} \frac{C_F \alpha_s}{\pi} \left(\ln \frac{\mu^2}{4m^2} + \frac{19}{12} - \frac{3\pi^2}{16} \right), \tag{37b}$$

where μ is now interpreted as the factorization scale in the $\overline{\rm MS}$ scheme. Note these coefficients are purely real.

With the knowledge of the $c_i^{(1)}$ in (37), we can employ (6) to determine the short-distance coefficients F and G that appear in (1) through order α_s:

$$\begin{aligned} F(^1S_0) &= \frac{m^2}{8\pi} \left[|c_0^{(0)}|^2 + 2{\rm Re}\left(c_0^{(0)} c_0^{(1)*} \right) + \mathcal{O}(\alpha_s^2) \right] \\ &= 2\pi e_Q^4 \alpha^2 \left[1 + \frac{C_F \alpha_s}{\pi} \left(\frac{\pi^2}{4} - 5 \right) + \mathcal{O}(\alpha_s^2) \right], \end{aligned} \tag{38a}$$

$$\begin{aligned} G(^1S_0) &= \frac{m^2}{4\pi} {\rm Re}\left[c_0^{(0)} c_2^{(0)*} + c_0^{(1)} c_2^{(0)*} + c_0^{(0)} c_2^{(1)*} + \mathcal{O}(\alpha_s^2) \right] \\ &= -\frac{8\pi e_Q^4 \alpha^2}{3} \left[1 + \frac{C_F \alpha_s}{\pi} \left(\frac{5\pi^2}{16} - \frac{49}{12} - \ln \frac{\mu^2}{4m^2} \right) + \mathcal{O}(\alpha_s^2) \right]. \end{aligned} \tag{38b}$$

The familiar result for $F(^1S_0)$ through $\mathcal{O}(\alpha_s)$ is then reproduced. The order-α_s correction to $G(^1S_0)$ is new, which constitutes the main result of this work.

To visualize the relative importance of these $\mathcal{O}(\alpha_s)$ corrections, one may choose $\mu = m$ in (38):

$$F(^1S_0) = 2\pi e_Q^4 \alpha^2 \left[1 - 3.38 \times \frac{\alpha_s(m)}{\pi} + \mathcal{O}(\alpha_s^2) \right], \tag{39a}$$

$$G(^1S_0) = -\frac{8\pi e_Q^4 \alpha^2}{3} \left[1 + 0.52 \times \frac{\alpha_s(m)}{\pi} + \mathcal{O}(\alpha_s^2) \right]. \tag{39b}$$

The order-α_s correction to $F(^1S_0)$ has modest effect for η_c decay to $\gamma\gamma$. If one takes $\alpha_s(m_c) = 0.3$, including this correction will reduce the tree-level value of F by about 30%. Nevertheless, the order-α_s correction to $G(^1S_0)$ seems to have a much minor impact, which only enhances the tree-level value of G roughly by 5% for $\mu = m$. Note even the relative sign of this correction is uncertain. If one instead chooses $\mu = 2m$, including this $\mathcal{O}(\alpha_s)$ correction would *reduce* the tree-level value of G by about 10%. It seems fair to state that, at current level of experimental accuracy, the $\mathcal{O}(\alpha_s)$ correction to $G(^1S_0)$ has very little phenomenological impact.

---

one again gets $C_q = \widetilde{C}_q = 0$ in q_4 scheme as before. However, for the q_D scheme in this case, one finds that $C_q = \widetilde{C}_q = -\frac{i\pi}{18v}$.

VII. SUMMARY

NRQCD factorization approach provides a model-independent framework for calculating the quarkonium annihilation decay rates. The nonperturbative NRQCD matrix elements are universal, which can be estimated from potential models or lattice QCD simulations, or directly fitted from experiments. On the contrary, being process-dependent, the short-distance coefficients appearing in the NRQCD factorization formula can be systematically improved in perturbation theory. To make a more precise prediction, it is desirable to know the short-distance coefficients at higher accuracy in α_s expansion.

In this work, we have computed the $\mathcal{O}(\alpha_s)$ corrections to the short-distance coefficients relevant to the process of pseudoscalar quarkonium decay to two photons. Specifically, we have deduced the $\mathcal{O}(\alpha_s)$ piece of the coefficient $G(^1S_0)$, which is associated with the relative order-v^2 NRQCD matrix element in (1). This coefficient is determined through equating the full QCD amplitude and the NRQCD amplitude for the quark process $Q\overline{Q}(^1S_0) \to \gamma\gamma$ through NLO in α_s and v^2. As a consistency check, it is found that the IR and Coulomb singularities, as well as those terms nonanalytic in $|\mathbf{q}|$, are exactly canceled upon matching the calculations on both sides. We have presented detailed descriptions for some subtle technical issues encountered in the calculation, such as consistent prescription for γ_5 in dimensional regularization, and the ambiguity about the dimensionality of relative momentum when projecting out the S-wave amplitude. We have explicitly verified that different artificial schemes in extracting the S-wave amplitude actually lead to the identical short-distance coefficients.

Although the $\mathcal{O}(\alpha_s v^2)$ correction appears to be phenomenologically insignificant for pseudoscalar quarkonium decay to two photons, it is of interest to investigate the analogous correction for the process of pseudoscalar quarkonium inclusive decay to light hadrons.

Note added in the proof. Shortly after this paper was sumbitted, a similar work has appeared in arXiv, which also addresses the $\mathcal{O}(\alpha_s v^2)$ correction to pseudoscalar quarkonium decay to two photons [37]. These authors performed the matching calculation directly at the decay rate level, and their final results agree with our (38).

Acknowledgments

This research was supported in part by the National Natural Science Foundation of China under grants No. 10875130, 10935012. The research of W. S. was also supported by Basic Science Research Program through the NRF of Korea funded by the MEST under contract No. 2011-0003023.

Appendix A: Useful one-loop scalar integrals

In this Appendix we tabulate those one-loop scalar integrals that are encountered in the calculation of the NLO QCD correction to the process $Q\overline{Q}(^1S_0^{[1]}) \to \gamma\gamma$. First we adopt the following definitions of the 2-, 3-, 4-point Passarino-Veltman scalar integrals [35]:

$$B_0(p_1^2; m_1^2, m_2^2) \equiv \frac{\mu^{2\epsilon}}{i\pi^{D/2}}\Gamma(1-\epsilon)\int d^D l\, \frac{1}{(l^2-m_1^2)((l+q_1)^2-m_2^2)}, \tag{A1a}$$

$$C_0(p_1^2, p_2^2, p_3^2; m_1^2, m_2^2, m_3^2) \equiv \frac{\mu^{2\epsilon}}{i\pi^{D/2}}\Gamma(1-\epsilon) \times \int d^D l\, \frac{1}{(l^2-m_1^2)((l+q_1)^2-m_2^2)((l+q_2)^2-m_3^2)}, \tag{A1b}$$

$$D_0(p_1^2, p_2^2, p_3^2, p_4^2; s_{12}, s_{23}; m_1^2, m_2^2, m_3^2, m_4^2) \equiv \frac{\mu^{2\epsilon}}{i\pi^{D/2}}\Gamma(1-\epsilon) \times \int d^D l\, \frac{1}{(l^2-m_1^2)((l+q_1)^2-m_2^2)((l+q_2)^2-m_3^2)((l+q_3)^2-m_4^2)}, \tag{A1c}$$

where the spacetime dimension $D = 4 - 2\epsilon$, $q_n = \sum_{i=1}^n p_i$ and $q_0 = 0$ and $s_{ij} = (p_i + p_j)^2$. The $i\epsilon$ prescription in each propagator has been tacitly assumed.

The desired results are:

$$B_0(-E^2 \pm 2k_1\cdot q + q^2; 0, m^2) = \frac{1}{\epsilon_{\rm UV}} + \ln\frac{\mu^2}{m^2} + 2 - \frac{2(E^2 \mp k_1\cdot q)\,\ln\frac{2(E^2\mp k_1\cdot q)}{m^2}}{2(E^2\mp k_1\cdot q) - m^2}, \tag{A2a}$$

$$C_0(0, m^2, -E^2 + q^2 \pm 2k_1\cdot q; m^2, m^2, 0) = \frac{{\rm Li}_2\left(\frac{-E^2+q^2\pm 2k_1\cdot q}{m^2}\right) - \frac{\pi^2}{6}}{2(E^2\mp k_1\cdot q)}, \tag{A2b}$$

$$C_0(4E^2, 0, 0; m^2, m^2, m^2) = \frac{1}{4E^2}\left(\frac{1}{2}\ln^2\frac{1+\beta}{1-\beta} - \frac{\pi^2}{2} - i\,\pi\ln\frac{1+\beta}{1-\beta}\right), \tag{A2c}$$

$$C_0(4E^2, m^2, m^2; m^2, m^2, 0) = \frac{1}{4E^2\beta}\left\{\left(\frac{1}{\epsilon_{\rm IR}} + \ln\frac{\mu^2}{m^2}\right)\left(-\ln\frac{1+\beta}{1-\beta} + i\,\pi\right) - \pi^2\right.$$
$$\left. + {\rm Li}_2\left(\frac{2\beta}{1+\beta}\right) - {\rm Li}_2\left(-\frac{2\beta}{1-\beta}\right) - i\,\pi\ln\frac{4\beta^2}{1-\beta^2}\right\}, \tag{A2d}$$

$$D_0(m^2, 0, 0, m^2; -E^2 + q^2 \pm 2k_1\cdot q, 4E^2; 0, m^2, m^2, m^2) = \frac{1}{8E^2(E^2\mp k_1\cdot q)\beta}$$
$$\times\left\{\left(\ln\frac{1+\beta}{1-\beta} - i\,\pi\right)\left(\frac{1}{\epsilon_{\rm IR}} + \ln\frac{\mu^2}{m^2} - 2\ln\frac{E^2\mp k_1\cdot q}{m^2} - \ln 4\beta^2\right) + \frac{\pi^2}{2}\right.$$
$$\left. + 2\left[{\rm Li}_2\left(\frac{1-\beta}{1+\beta}\right) - {\rm Li}_2\left(-\frac{1-\beta}{1+\beta}\right)\right]\right\}. \tag{A2e}$$

All the involved kinematic factors, such as k_1, q, E, β, have already been defined in Section III A. The dilogarithm is defined through

$${\rm Li}_2(x) = -\int_0^x dt\,\frac{\ln(1-t)}{t}. \tag{A3}$$

All the infrared divergent one-loop scalar integrals (up to 4-point) have been classified in Ref. [35], which also compiles the corresponding analytic expressions. We thus can directly deduce the analytic expressions (A2d) and (A2e) from [35] by making appropriate substitutions. The analytic expression for the Coulomb-divergent three-point integral, (A2d), is well known and can be found in many places, *e.g.*, Eq. (4.14) in [35], or Eq. (B10) in [23]. However, if one starts from Eq. (4.47) of [35] to deduce the Coulomb-divergent D_0 function, one would unfortunately end up with an erroneous expression for the imaginary part. In (A2e), we present the correct analytic expression for the imaginary part, which is derived by employing the D-dimensional Cutkosky's rule. Its correctness has been numerically verified with the help of the MATHEMATICA package LOOPTOOLS [36].

[1] T. Appelquist and H. D. Politzer, Phys. Rev. Lett. **34**, 43 (1975).

[2] A. De Rujula and S. L. Glashow, Phys. Rev. Lett. **34**, 46 (1975).

[3] R. Barbieri, R. Gatto and R. Kogerler, Phys. Lett. B **60**, 183 (1976).

[4] V. A. Novikov, L. B. Okun, M. A. Shifman, A. I. Vainshtein, M. B. Voloshin and V. I. Zakharov, Phys. Rept. **41**, 1 (1978).

[5] G. T. Bodwin, E. Braaten and G. P. Lepage, Phys. Rev. D **51**, 1125 (1995) [Erratum-ibid. D **55**, 5853 (1997)] [arXiv:hep-ph/9407339].

[6] D. Ebert, R. N. Faustov and V. O. Galkin, Mod. Phys. Lett. A **18**, 601 (2003) [arXiv:hep-ph/0302044].

[7] J. P. Lansberg and T. N. Pham, Phys. Rev. D **74**, 034001 (2006) [arXiv:hep-ph/0603113].

[8] M. Z. Yang, Phys. Rev. D **79**, 074026 (2009) [arXiv:0902.1295 [hep-ph]].

[9] G. T. Bodwin and A. Petrelli, Phys. Rev. D **66**, 094011 (2002) [arXiv:hep-ph/0205210].

[10] N. Brambilla, E. Mereghetti and A. Vairo, JHEP **0608**, 039 (2006) [arXiv:hep-ph/0604190].

[11] I. Harris and L. M. Brown, Phys. Rev. **105**, 1656 (1957).

[12] R. Barbieri, E. d'Emilio, G. Curci and E. Remiddi, Nucl. Phys. B **154**, 535 (1979).

[13] K. Hagiwara, C. B. Kim and T. Yoshino, Nucl. Phys. B **177**, 461 (1981).

[14] A. Czarnecki and K. Melnikov, Phys. Lett. B **519**, 212 (2001) [arXiv:hep-ph/0109054].

[15] W. Y. Keung and I. J. Muzinich, Phys. Rev. D **27**, 1518 (1983).

[16] Z. G. He, Y. Fan and K. T. Chao, Phys. Rev. D **75**, 074011 (2007) [arXiv:hep-ph/0702239].

[17] G. T. Bodwin, H. S. Chung, D. Kang, J. Lee and C. Yu, Phys. Rev. D **77**, 094017 (2008) [arXiv:0710.0994 [hep-ph]].

[18] H. S. Chung, J. Lee and C. Yu, Phys. Lett. B **697**, 48 (2011) [arXiv:1011.1554 [hep-ph]].

[19] C. Amsler *et al.* [Particle Data Group Collaboration], Phys. Lett. **B667**, 1-1340 (2008).

[20] K. Nakamura *et al.* [Particle Data Group Collaboration], J. Phys. G **G37**, 075021 (2010).

[21] M. E. Luke and M. J. Savage, Phys. Rev. D **57**, 413 (1998) [arXiv:hep-ph/9707313].

[22] M. Beneke and V. A. Smirnov, Nucl. Phys. B **522**, 321 (1998).

[23] G. T. Bodwin, H. S. Chung, J. Lee and C. Yu, Phys. Rev. D **79**, 014007 (2009) [arXiv:0807.2634 [hep-ph]].

[24] J. Lee, W. Sang and S. Kim, JHEP **1101**, 113 (2011) [arXiv:1011.2274 [hep-ph]].

[25] M. S. Chanowitz, M. Furman and I. Hinchliffe, Nucl. Phys. B **159**, 225 (1979).

[26] J. G. Korner, D. Kreimer and K. Schilcher, Z. Phys. C **54**, 503 (1992).

[27] G. 't Hooft and M. J. G. Veltman, Nucl. Phys. B **44**, 189 (1972).

[28] P. Breitenlohner and D. Maison, Commun. Math. Phys. **52**, 11 (1977).

[29] A. Petrelli, M. Cacciari, M. Greco, F. Maltoni and M. L. Mangano, Nucl. Phys. B **514**, 245 (1998) [arXiv:hep-ph/9707223].

[30] E. Braaten and Y. Q. Chen, Phys. Rev. D **54**, 3216 (1996) [arXiv:hep-ph/9604237].

[31] E. Braaten and Y. Q. Chen, Phys. Rev. D **55**, 2693 (1997) [arXiv:hep-ph/9610401].

[32] T. H. West, Comput. Phys. Commun. **77**, 286 (1993).

[33] R. Mertig, M. Bohm and A. Denner, Comput. Phys. Commun. **64**, 345 (1991).

[34] G. T. Bodwin, J. Lee and C. Yu, Phys. Rev. D **77**, 094018 (2008) [arXiv:0710.0995 [hep-ph]].

[35] R. K. Ellis and G. Zanderighi, JHEP **0802**, 002 (2008) [arXiv:0712.1851 [hep-ph]].

[36] T. Hahn and M. Perez-Victoria, Comput. Phys. Commun. **118**, 153 (1999).

[37] H. K. Guo, Y. Q. Ma and K. T. Chao, arXiv:1104.3138 [hep-ph].